Electronic Energy Migration and Trapping in Quinone-Substituted, Phenyl-Linked Dimeric and Trimeric Porphyrins

Jonathan L. Sessler,*,† Vincent L. Capuano,† and Anthony Harriman*,‡

Contribution from the Department of Chemistry and Biochemistry and the Center for Fast Kinetics Research, The University of Texas at Austin, Austin, Texas 78712

Received November 9, 1992

Abstract: The synthesis and photophysical characterization of a series of quinone-substituted, phenyl-linked dimeric and trimeric porphyrin arrays suitable for the study of electron transfer within closely-coupled subunits is presented. The excited singlet state of a porphyrin possessing a quinone substituent at a *meso* position is shortened to <350 fs due to electron donation to the appended quinone. Energy transfer between adjacent porphyrins occurs with a rate constant of ca. 10^{11} s^{-1}, and the photon is immediately trapped by the proximal porphyrin. For the linear porphyrin trimer, the photon can transfer between distal and central porphyrins in an incoherent manner until it is trapped by the proximal porphyrin. These arrays represent interesting models for natural photosynthetic organisms since they combine light harvesting, energy migration and trapping, and photoinduced electron transfer in a single supramolecular entity.

Introduction

Supramolecular chemistry[1] and molecular engineering[2] have reached levels of sophistication where the cooperative behavior of individual subunits within a controlled spatial assembly can be examined in detail. The potential application of these approaches to the design of molecular systems capable of self-replication[3] and solar energy conversion[4] as well as to the design of nanoscale machinery,[5] however, is still in its infancy. A natural approach to the development of artificial systems capable of performing specific functions, therefore, is to mimic the essential features employed by living systems in carrying out the desired task. The recent advances in the chemistry of self-replication,[3] where the molecular recognition and templating motifs of cellular replication are being applied to wholly synthetic systems, are a clear example. Similarly, much of what is known in the area of supramolecular photochemistry[6] is due to the study and mimicry of the primary events occurring within the reaction centers (RC's) of photosynthetic bacteria.[7,8]

The initial events occurring within the RC's are photoinduced long-distance electron-transfer (ET) reactions. These proteins make use of an array of electronically coupled tetrapyrrolic macrocycles[9] to effect long-range charge separation with a quantum yield approaching unity. A wealth of kinetic data obtained from time-resolved optical[10,11] and magnetic[12] spectroscopic studies performed on native and modified RC's has served to elucidate the mechanisms and dynamics of ET within these

† Department of Chemistry and Biochemistry.

‡ Center for Fast Kinetics Research.

(1) Lehn, J.-M. *Angew. Chem., Int. Ed. Engl.* **1988**, *27*, 90–112; *Angew. Chem.* **1988**, *100*, 91–113.

(2) (a) Haddon, R. C.; Lamola, A. A. *Proc. Natl. Acad. Sci. U.S.A.* **1985**, *82*, 1874–1878. (b) Drexler, K. E. *Proc. Natl. Acad. Sci. U.S.A.* **1981**, *78*, 5275–5278. (c) *Molecular Electronic Devices*; Carter, F., Ed.; Marcel Dekker: New York, 1982. (d) *Molecular Electronic Devices II*; Carter, F., Ed.; Marcel Dekker: New York, 1987.

(3) (a) Kiedrowski, G. V.; Wlotzka, B.; Helbing, J.; Matzen, M.; Jordan, S. *Angew. Chem., Int. Ed. Engl.* **1991**, *30*, 423–426; *Angew. Chem.* **1990**, *103*, 456–459. (b) Rebek, J., Jr. *Angew. Chem., Int. Ed. Engl.* **1990**, *29*, 245–255; *Angew. Chem.* **1990**, *100*, 91–113. (c) Tjivikua, T.; Ballester, P.; Rebek, J., Jr. *J. Am. Chem. Soc.* **1990**, *112*, 1249–1250. (d) Rebek, J., Jr. *Science* **1987**, *235*, 1478–1484. (e) Kiedrowski, G. V. *Angew. Chem., Int. Ed. Engl.* **1986**, *25*, 932–935; *Angew. Chem.* **1986**, *98*, 932–934.

(4) (a) Scandola, F.; Indelli, M. T.; Chiorboli, C.; Bignozzi, C. A. *Top. Curr. Chem.* **1990**, *158*, 73–149. (b) Meyer, T. J. *Acc. Chem. Res.* **1989**, *22*, 163–170. (c) Wasielewski, M. R. In *Photoinduced Electron Transfer*, Part A; Fox, M. A., Chanon, M., Eds.; Elsevier: Amsterdam, 1988; pp 161–206.

(5) (a) Anelli, P. L.; Ashton, P. R.; Ballardini, R.; Balzani, V.; Delgado, M.; Gandolfi, M. T.; Goodnow, T. T.; Kaifer, A. E.; Philp, D.; Pietrasziewicz, M.; Prodi, L.; Reddington, M. V.; Slawin, A. M. Z.; Spencer, N.; Stoddart, J. F.; Vicent, C.; Williams, D. J. *J. Am. Chem. Soc.* **1992**, *114*, 193–218 and references cited therein. (b) Kaszynski, P.; Friedli, A. C.; Michl, J. *J. Am. Chem. Soc.* **1992**, *114*, 601–620 and references cited therein. (c) Stoddart, J. F.; Mathias, J. P.; Kohnke, F. H. *Angew. Chem. Adv. Mater.* **1989**, *101*, 1129–1136.

(6) (a) Fox, M. A., Chanon, M., Eds. *Photoinduced Electron Transfer*; Elsevier: Amsterdam, 1988. (b) Balzani, V., Ed. *Supramolecular Photochemistry*; NATO ASI Series; D. Reidel: Dordrecht, The Netherlands, 1987.

(7) (a) Deisenhofer, J.; Epp, O.; Miki, K.; Huber, R.; Michel, H. *Nature* **1985**, *318*, 618–624. (b) Feher, G.; Allen, J. P.; Okamura, M. Y.; Rees, D. C. *Nature* **1989**, *339*, 111–116.

(8) (a) Bolton, J. R., Mataga, N., McLendon, G., Eds. *Electron Transfer in Inorganic, Organic, and Biological Systems*; Advances in Chemistry 228; American Chemical Society: Washington, DC, 1991. (b) Palmer, G. A., et al., Eds. *Long Range Electron Transfer in Biology*; Structure and Bonding 75; Springer: Berlin, 1991. (c) Johnson, M. K., et al., Eds. *Electron Transfer in Biology and the Solid State*; Advances in Chemistry 226; American Chemical Society: Washington, DC, 1990.

(9) Structural information from X-ray diffraction experiments is available for the photosynthetic bacteria *Rhodopseudomonas viridis* and *R. Sphaeroides* (see ref 7). These membrane-bound proteins contain four bacteriochlorophylls (BChl), two bacteriopheophytins (BPh) (structurally identical with the BChl except that the central magnesium ion is replaced with two hydrogen atoms), and two quinones (Q_A, tightly associated; Q_B, weakly associated). Two of the BChl are held in close proximity by the protein matrix so that they behave as a dimer $(BChl)_2$ often referred to as the "special pair". The remaining vectorial ET pathway consists of a monomeric BChl and a monomeric BPh which forms a bridge between the initial electron donor $(BChl)_2$ and acceptor Q_A.

(10) (a) Moser, C. C.; Keske, J. M.; Warncke, K.; Farid, R. S.; Dutton, P. L. *Nature* **1992**, *355*, 796–802. (b) Bixon, M.; Jortner, J.; Michel-Beyerle, M. E. In *Reaction Centers of Photosynthetic Bacteria*; Michel-Beyerle, M. E., Ed.; Springer: Berlin, 1991; pp 157–168. (c) Freisner, R. A.; Won, Y. *Biochim. Biophys. Acta* **1989**, *977*, 99–122. (d) Holzapfel, W.; Finkele, U.; Kaiser, W.; Oesterhelt, D.; Scheer, H.; Stiltz, H. U.; Zinth, W. *Chem. Phys. Lett.* **1989**, *160*, 1–7. (e) Johnson, S. G.; Tang, D.; Jankowiak, R.; Hayes, J. M.; Small, G. J.; Tiede, D. M. *J. Phys. Chem.* **1989**, *93*, 5953–5957. (f) Fleming, G. R.; Martin, J. L.; Breton, J. *Nature* **1988**, *333*, 190–192. (g) Tang, D.; Jankowiak, R.; Gillie, J. K.; Small, G. J.; Tiede, D. M. *J. Phys. Chem.* **1988**, *92*, 4012–4015. (h) Breton, J.; Martin, J.-L.; Fleming, G. R.; Lambry, J.-C. *Biochemistry* **1988**, *27*, 8276–8284. (i) Marcus, R. A. *Chem. Phys. Lett.* **1987**, *133*, 471–477. (j) Martin, J.-L.; Breton, J.; Hoff, A. J.; Migus, A.; Antonetti, A. *Proc. Natl. Acad. Sci. U.S.A.* **1986**, *83*, 957–961. (k) Wasliewski, M. R.; Tiede, D. M. *FEBS Lett.* **1986**, *204*, 368–372. (l) Woodbury, N. W.; Becker, M.; Middendorf, D.; Parson, W. W. *Biochemistry* **1985**, *24*, 201–203.

0002-7863/93/1515-4618$04.00/0

membrane-bound proteins. In addition, a number of model studies[13] incorporating derivatized porphyrins (modeled after the bacteriochlorophylls and bacteriopheophytins of the RC) have been undertaken in an attempt to understand the charge-separation process[14] and/or to achieve long-lived redox products.[13,15] In particular, Gust and Moore[13d,15] have achieved significant success with multi-porphyrin systems in which electronic coupling between subunits is weak. By contrast, there have been few reports of multi-porphyrin systems composed of strongly-coupled subunits which demonstrate photoinduced ET.[16-18] Such systems may be useful for examining the dependence of ET rates on intrasubunit interactions and also for designing supramolecular systems capable of sequential energy-transfer steps between porphyrins prior to ET. With this in mind, we now provide full details of the synthesis and photophysical characterization of a series of quinone-substituted, phenyl-linked porphyrin trimers **1**–**3** suitable for the study of ET within a system of highly-coupled photoactive subunits.[17] In trimer **2**, the most

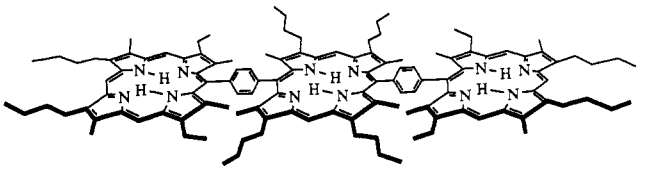

1

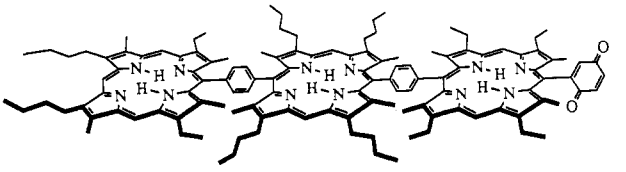

2

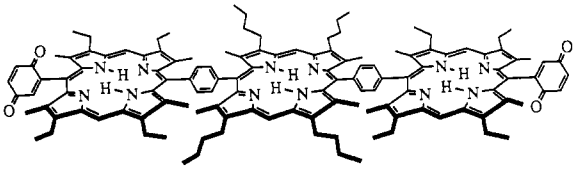

3

elaborate of these models, the distant (distal) porphyrin-to-quinone center-to-center distance is estimated to be 32.0 Å (26.8 Å edge-to-edge) as extrapolated from X-ray structural data obtained with monomeric and dimeric models;[18] the corresponding center-to-center inter-porphyrin distances are estimated to be 12.8 and 25.5 Å (5.86 and 19.9 Å edge-to-edge) between adjacent and once-removed porphyrin subunits, respectively.

In order to understand the various events which follow from excitation of these trimers, we have studied also the photophysical properties of the quinone-containing porphyrin dimer **4** and the

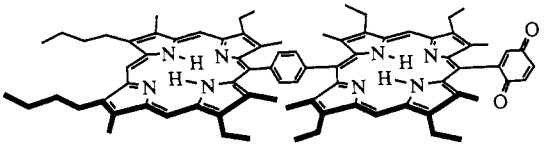

4

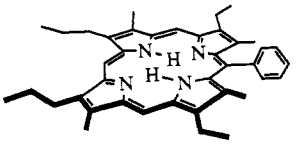

5

unsubstituted monomer **5**.[18] It was observed that rapid energy transfer occurs between porphyrin subunits within these phenyl-linked supramolecular arrays but that this process is slow with respect to electron transfer between a directly-linked porphyrin–quinone couple. Thus, the trimeric array acts as a minute light-harvesting antenna for the porphyrin adjacent to the quinone. In this respect, arrays such as **2** represent simple models for the natural photosynthetic apparatus since they possess the key features of light harvesting, energy transfer and trapping, and photoinduced ET in a single entity.

Results and Discussion

Synthesis of Trimeric Porphyrin Arrays. The new compounds reported here for the first time (**2**) or in full detail (**1** and **3**) were prepared using a modification of the preparative sequence reported

(11) For discussions of the "superexchange" mechanism as it relates to RC photochemistry, see: (a) Bixon, M.; Jortner, J.; Michel-Beyerle, M. E. In *Reaction Centers of Photosynthetic Bacteria*; Michel-Beyerle, M. E., Ed.; Springer: Berlin, 1991; pp 157–168. (b) Bixon, M.; Jortner, J. *Chem. Phys. Lett.* **1989**, *159*, 17–20. (c) Bixon, M.; Jortner, J.; Michel-Beyerle, M. E.; Ogrodnik, A. *Biochim. Biophys. Acta* **1989**, *977*, 273–286. (d) Friesner, R. A.; Won, Y. *Biochim. Biophys. Acta* **1989**, *977*, 99–122. (e) Hu, Y.; Mukamel, S. *Chem. Phys. Lett.* **1989**, *160*, 410–416. (f) Won, Y.; Friesner, R. A. *Biochim. Biophys. Acta* **1988**, *935*, 9–18. (g) Michel-Beyerle, M. E.; Plato, M.; Deisenhofer, J.; Michl, H.; Bixon, M.; Jortner, J. *Biochim. Biophys. Acta* **1988**, *932*, 52–70. (h) Michel-Beyerle, M. E.; Bixon, M.; Jortner, J. *Chem. Phys. Lett.* **1988**, *151*, 188–194. (i) Bixon, M.; Jortner, J. *J. Phys. Chem.* **1988**, *92*, 7148–7156. (j) Plato, M.; Mobius, K.; Michel-Beyerle, M. E.; Bixon, M.; Jortner, J. *J. Am. Chem. Soc.* **1988**, *110*, 7279–7285. (k) Marcus, R. A. *Chem. Phys. Lett.* **1987**, *133*, 471–477. (l) Won, Y.; Friesner, R. A. *Proc. Natl. Acad. Sci. U.S.A.* **1987**, *84*, 5511–5515. (m) Ogrodnik, A.; Remy-Richter, N.; Michel-Beyerle, M. E.; Feick, R. *Chem. Phys. Lett.* **1987**, *135*, 576–581. (n) Bixon, M.; Jortner, J.; Michel-Beyerle, M. E.; Ogrodnik, A.; Lersch, W. *Chem. Phys. Lett.* **1987**, *140*, 626–630. (o) Bixon, M.; Jortner, J. *J. Phys. Chem.* **1986**, *90*, 3795–3800.

(12) (a) Boxer, S. G.; Goldstein, R. A.; Lockhart, D. J.; Middendorf, T. R.; Takiff, L. *J. Phys. Chem.* **1989**, *93*, 8280–8294. (b) Lockhart, D. J.; Boxer, S. G. *Chem. Phys. Lett.* **1988**, *144*, 243–250. (c) Lockhart, D. J.; Boxer, S. G. *Proc. Natl. Acad. Sci. U.S.A.* **1988**, *85*, 107–111. (d) Lockhart, D. J.; Boxer, S. G. *Biochemistry* **1987**, *26*, 664–668. (e) Boxer, S. G.; Lockhart, D. J.; Middendorf, T. R. *Chem. Phys. Lett.* **1986**, *123*, 476–482.

(13) For recent reviews, see: (a) Wasielewski, M. R. *Chem. Rev.* **1992**, *92*, 435–461. (b) *Tetrahedron* **1989**, *45*(*15*) (a special "Symposium in Print" issue devoted to the topic of covalently linked donor–acceptor photosynthetic model systems, Gust, D. A., Moore, T. A., Eds.). (c) Connolly, J. S.; Bolton, J. R. In *Photoinduced Electron Transfer*, Part D; Fox, M. A., Chanon, M., Eds.; Elsevier: Amsterdam, 1988; pp 303–393. (d) Gust, D.; Moore, T. A. *Science* **1989**, *244*, 35–41.

(14) (a) Aoyama, Y.; Asakawa, M.; Matsui, Y.; Ogoshi, H. *J. Am. Chem. Soc.* **1991**, *113*, 6233–6240. (b) Bolton, J. R. In *Electron Transfer in Inorganic, Organic, and Biological Systems*; Bolton, J. R., Mataga, N., McLendon, G., Eds.; Advances in Chemistry 228; American Chemical Society: Washington, DC, 1991; pp 117–131. (c) Osuka, A.; Maruyama, K.; Yamazaki, I.; Tamai, N. *Chem. Phys. Lett.* **1990**, *165*, 392–396. (d) Anderson, H. L.; Hunter, C. A.; Sanders, J. K. M. *J. Chem. Soc., Chem. Commun.* **1989**, 226–227. (e) Hunter, C. A.; Meah, M. N.; Sanders, J. K. M. *J. Chem. Soc., Chem. Commun.* **1988**, 694–696. (f) Joran, A. D.; Leland, B. A.; Felker, P. M.; Zewail, A. H.; Hopfield, J. J.; Dervan, P. B. *Nature (London)* **1987**, *327*, 508–511. (g) Cowan, J. A.; Sanders, J. K. M.; Beddard, G. S.; Harrison, R. J. *J. Chem. Soc., Chem. Commun.* **1987**, 55–58. (h) Leland, B. A.; Joran, A. D.; Felker, P. M.; Hopfield, J. J.; Zewail, A. H.; Dervan, P. B. *J. Phys. Chem.* **1985**, *89*, 5571–5573. (i) Wasieleski, M. R.; Niemczyk, M. P.; Svec, W. A.; Pewitt, E. B. *J. Am. Chem. Soc.* **1985**, *107*, 5562–5563. (j) Sakata, Y.; Nishitani, S.; Nishimizu, N.; Misumi, S.; McIntosh, A. R.; Bolton, J. R.; Kanda, Y.; Karen, A.; Okada, T.; Mataga, N. *Tetrahedron Lett.* **1985**, 5207–5210. (k) Joran, A. D.; Leland, B. A.; Geller, G. G.; Hopfield, J. J.; Dervan, P. B. *J. Am. Chem. Soc.* **1984**, *106*, 6090–6092.

(15) (a) Gust, D.; Moore, T. A. *Adv. Photochem.* **1991**, *16*, 1–65. (b) Gust, D.; Moore, T. A. *Top. Curr. Chem.* **1991**, *159*, 103.

(16) (a) Osuka, A.; Nagata, T.; Maruyama, K. *Chem. Lett.* **1991**, 481–484. (b) Nagata, T.; Osuka, A.; Maruyama, K. *J. Am. Chem. Soc.* **1990**, *112*, 3054–3059. (c) Chardon-Noblat, S.; Sauvage, J.-P.; Mathis, P. *Angew. Chem., Int. Ed. Engl.* **1989**, *28*, 593–594. (d) Heiler, D.; McLendon, G. L.; Rogalskyj, P. *J. Am. Chem. Soc.* **1987**, *109*, 604–606.

(17) (a) Sessler, J. L.; Capuano, V. L. *Angew. Chem.* **1990**, *102*, 1162–1165; *Angew. Chem., Int. Ed. Engl.* **1990**, *29*, 1134–1137. (b) Sessler, J. L.; Capuano, V. L.; Kubo, Y.; Johnson, M. R.; Magda, D. J.; Harriman, A. In *Photoprocesses in Transition Metal Complexes, Biosystems and Other Molecules*; Kochanski, E., Ed.; Kluwer: New York, in press.

(18) (a) Sessler, J. L.; Johnson, M. R.; Creager, S. E.; Fettinger, J. C.; Ibers, J. A. *J. Am. Chem. Soc.* **1990**, *112*, 9310–9329. (b) Rodriguez, J.; Kirmaier, C.; Johnson, M. R.; Freisner, R. A.; Holten, D.; Sessler, J. L. *J. Am. Chem. Soc.* **1991**, *113*, 1652–1659.

Scheme I

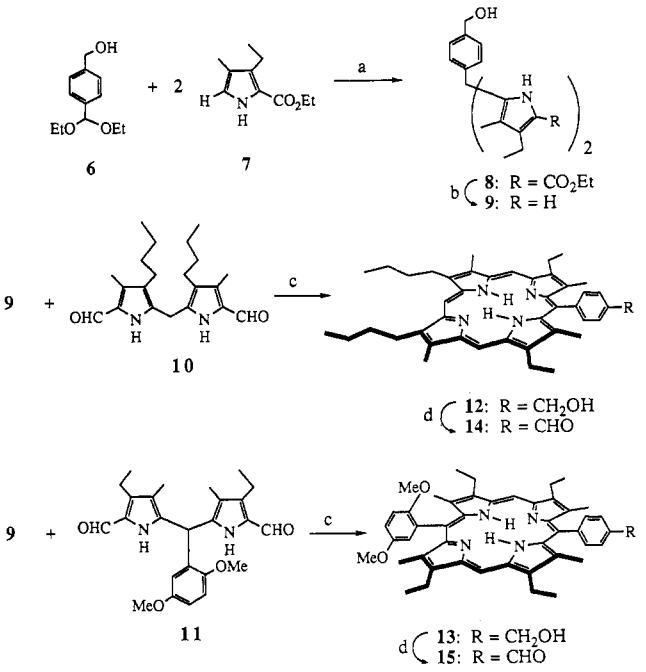

(a) HCl (cat.), ethanol, reflux, 12 h. (b) (i) NaOH (3–10 equiv), ethanol:H_2O (95:5), reflux, $^1/_2$ h; (ii) ethylene glycol, 195 °C, 2 h. (c) (i) $HClO_4$ (cat.), THF:methanol (2:1), 25 °C, 12–16 h; (ii) *o*-chloranil. (d) PdC (2–5 equiv), CH_2Cl_2, 4–8 h.

by Chang and Abdalmuhdi[19] for the synthesis of a stacked, anthracene-linked trimeric porphyrin. This strategy[16a,b] involves synthesis of the "outer porphyrin" aryl aldehyde precursors with the "central porphyrin" being constructed in the final bond-forming sequence. It thus rests on the availability of the appropriate pyrrole and dipyrrylmethane starting materials. The sequence followed in the preparation of these "building blocks" is shown in Scheme I. The key pyrrole **7** and the dipyrrylmethanes **10** and **11** have been prepared previously in our laboratory[18,20] and elsewhere.[21]

With pyrrole **7**, several phenyldipyrrylmethanes can be obtained by acid-catalyzed condensation with the appropriate aryl aldehyde. Accordingly, compound **8** was prepared by the acid-catalyzed reaction of **7** with 4-(hydroxymethyl)benzaldehyde (generated *in situ* from the corresponding diethyl acetal **6**), in 75% yield. The resulting dipyrrylmethane ester, **8**, was then saponified and decarboxylated using a method reported previously[22] to give compound **9** in 95% yield (based on **6**). The functionalized porphyrin monomers **12–15** were prepared by literature methods.[18,20,22,23]

The route to the trimeric porphyrins **1–3** is based on the condensation between the dipyrrylmethane **16**, which is unsubstituted at the 5,5′-position, and the porphyrin aldehydes **14** and **15**. We have employed a modification of the original approach of Chang[19] based on the optimized conditions introduced by

Scheme II

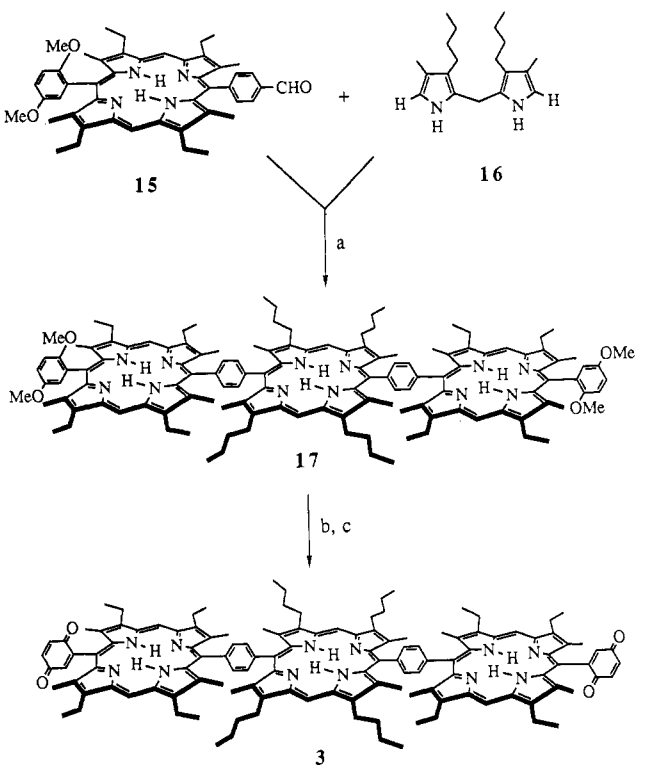

(a) (i) **15** (0.02 M), **16** (0.02 M), TFA (mM), CH_2Cl_2, 25 °C, $3^1/_2$ h; (ii) *o*-chloranil (3–6 equiv), 40 °C, 1–3 h. (b) BI_3 (5–10 equiv), CH_2Cl_2, 0 °C, $^1/_2$ h. (c) DDQ, CH_2Cl_2, 5 min.

Lindsey[24] in the context of porphyrinogen-based tetraphenylporphyrin syntheses. The synthetic strategy developed by Lindsey takes advantage of the greater equilibrium stability of cyclic porphyrinogens over open-chain polypyrrylmethanes at moderate dilution. We anticipated the same type of equilibrium situation in the formation of 5,15-diarylporphyrins from aryl aldehydes and 5,5′-diunsubstituted dipyrrylmethanes. By employing Lindsey's conditions (0.01 M reactants, 1–10 mM trifluoroacetic acid (TFA), CH_2Cl_2, 25 °C, $3^1/_2$ h), we have been able to isolate trimeric porphyrins routinely in >50% yield, and in some cases as high as 80%. This is not surprising when one considers that the use of dipyrrylmethanes and aryl aldehydes requires the formation of half the number of C–C bonds as the original Lindsey procedure involving monomeric pyrroles. These optimized conditions are outlined in the synthetic sequence of Scheme II for the specific trimer-forming case associated with the preparation of the bis-quinone trimer **3**. In this case, the critical condensation gives the protected bis-hydroquinone methyl ether **17** (51% yield). Demethylation of this intermediate, **17**, with BBr_3 (or BI_3)[25] and subsequent oxidation with 2,3-dichloro-5,6-dicyano-1,4-benzoquinone (DDQ)[26] afforded **3** in 40–50% yield following chromatographic purification (silica gel, 2% $CH_3OH/CHCl_3$ eluent).

The synthesis of trimer **1** was achieved in an analogous manner by substituting porphyrin aldehyde **14** for precursor **15**. Finally, under the reaction conditions described, a 1:1:1 mixture of precursors **14**, **15**, and **16** reacted to give compounds **1**, **17**, and **18** in a roughly 1:1:2 ratio (Scheme III). This mixture was separated by careful chromatography on silica gel (see the Experimental Section). Compound **18**, the protected monohydroquinone ether porphyrin trimer, obtained in 23% yield

(19) Abdalmuhdi, I.; Chang, C. K. *J. Org. Chem.* **1985**, *50*, 411–413.
(20) Sessler, J. L.; Hugdahl, J.; Johnson, M. R. *J. Org. Chem.* **1986**, *51*, 2838–2840 and references cited therein.
(21) Chang, C. K.; Abdalmuhdi, I. *J. Org. Chem.* **1983**, *48*, 5388–5390. For lead references on pyrrole and dipyrrylmethane chemistry, see: (a) Kim, J. B.; Adler, A. D.; Longo, F. R. In *The Porphyrins*; Dolphin, D., Ed.; Academic: New York, 1978; Vol. 1, Part A, pp 85–99. (b) Paine, J. B. In *The Porphyrins*; Dolphin, D., Ed.; Academic: New York, 1978; Vol. 1, Part A, pp 101–123.
(22) (a) Chang, C. K.; Abdalmuhdi, I. *Angew. Chem., Int. Ed. Engl.* **1984**, *23*, 164–165. (b) Abdalmuhdi, I.; Chang, C. K. *J. Org. Chem.* **1985**, *50*, 411–413. (c) Eaton, S. S.; Eaton, G. R.; Chang, C. K. *J. Am. Chem. Soc.* **1985**, *107*, 3177–3184.
(23) (a) Arsenault, G. P.; Bullock, E.; MacDonald, S. F. *J. Am. Chem. Soc.* **1960**, *82*, 4384–4396.
(24) Lindsey, J. S.; Schreiman, I. C.; Hsu, H. C.; Kearney, P. C.; Marguerettaz, A. M. *J. Org. Chem.* **1987**, *52*, 827–836.
(25) *Protective Groups in Organic Synthesis*; Greene, T. W., Wuts, P. G. M., Eds.; Wiley: New York, 1990; pp 146–149.
(26) Turner, T. In *Synthetic Reagents*; Pizey, M., Ed.; Wiley: New York, 1977; Vol. 3, pp 193–225.

Scheme III

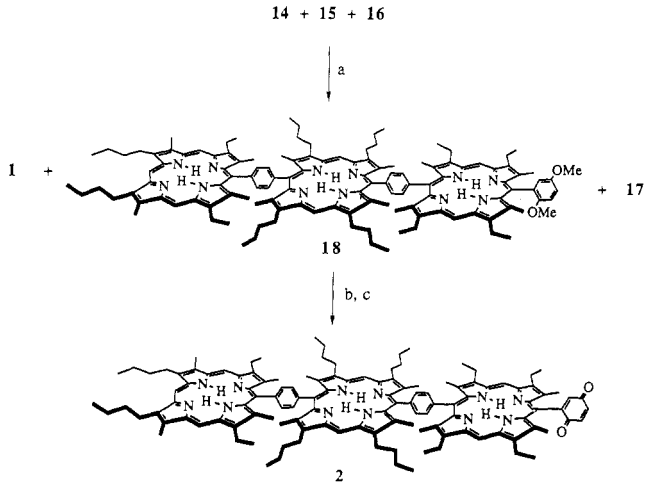

(a) (i) **14** (0.01 M), **15** (0.01 M), **16** (0.02 M), TFA (mM), CH_2Cl_2, 25 °C, $3^1/_2$ h; (ii) *o*-chloranil (3–6 equiv), 40 °C, 1–3 h. (b) BI_3 (5–10 equiv), CH_2Cl_2, 0 °C, $^1/_2$ h. (c) DDQ, CH_2Cl_2, 5 min.

following such purification, was then treated with BBr_3 in CH_2Cl_2 and oxidized with DDQ to yield the desired monoquinone porphyrin trimer **2**.

Photophysics of Quinone-Free Porphyrin Arrays. The optical properties of porphyrin arrays are of interest in terms of the electronic coupling between porphyrin subunits. Spectral shifts associated with electronic coupling between porphyrin subunits have been described previously in terms of Kasha's molecular exciton model[27] and applied to phenyl-linked porphyrin arrays.[16b,28,29] Absorption spectra for trimer **1** and **2** and the prototypical monomer **5** in benzene solution are shown in Figure 1. This comparison reveals that the three porphyrin subunits of **1** and **2** do not act as isolated porphyrins. The four-banded (D_{2h}-type) visible spectra are broadened with respect to that of the monomer, as evidenced by overlap of the $Q_x(1,0)$ and $Q_y(1,0)$ bands in the trimers. A comparison of the Soret bands for these three compounds is presented in Figure 2. These transitions in the trimeric compounds are broadened and red-shifted relative to that of the monomer. This effect has been ascribed to optical coupling in other rigidly-linked porphyrin dimers, trimers, and higher oligomers.[16b,28,29]

Fluorescence spectra recorded for the trimers were red-shifted by ca. 200 cm^{-1} and somewhat broadened relative to that of the monomer (Figure 3). The triplet–triplet absorption spectrum recorded for trimer **1** was also distorted relative to that of the monomer **5** (Figure 4). These spectral changes serve to indicate that exciton coupling is preserved in the lowest energy excited singlet and triplet states. Indeed, analysis of the Q_y absorption transitions for **1** in a low-temperature glass indicated that the exciton coupling energy (V) was 45 ± 5 cm^{-1}. A slightly lower value (V = 40 ± 5 cm^{-1}) was derived for the quinone-substituted trimer **2**. These values are ca. 30-fold smaller than the corresponding values for the Soret transitions and were observed to increase slightly with increasing solvent polarity.[30] Although modest in magnitude, this electronic coupling between the porphyrin subunits is considered to be significant. This is because it may be taken to indicate moderately high through-bond interactions between porphyrin nuclei.

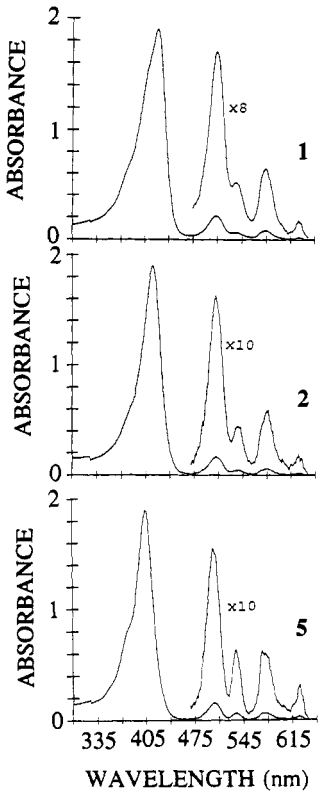

Figure 1. Absorption spectra recorded in benzene solution for trimer **1**, monoquinone-substituted trimer **2**, and unsubstituted monomer **5**.

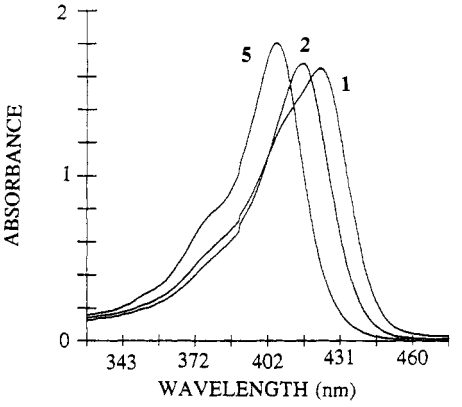

Figure 2. Comparison of the Soret transitions for trimer **1**, monoquinone-substituted trimer **2**, and unsubstituted monomer **5**.

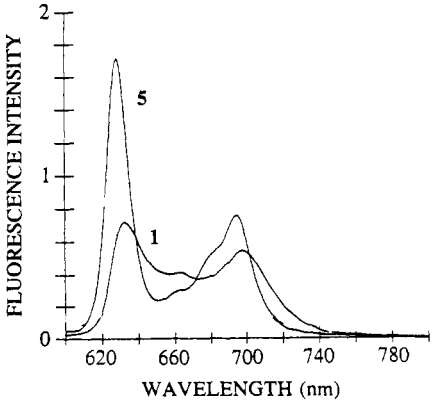

Figure 3. Steady-state fluorescence spectra recorded in benzene solution for trimer **1** and unsubstituted monomer **5**.

(27) Kasha, M.; Rawls, H. R.; El Bayoumi, M. A. *Pure Appl. Chem.* **1989**, *22*, 371–392.

(28) Won, Y.; Friesner, R. A.; Johnson, M. R.; Sessler, J. L. *Photosynth. Res.* **1989**, *22*, 201–210.

(29) (a) Schick, G. A.; Schreiman, I. C.; Wagner, R. W.; Lindsey, J. S.; Bocian, D. F. *J. Am. Chem. Soc.* **1989**, *111*, 1344–1350. (b) Maltzan, B. V. *Z. Naturforsch., A: Phys., Phys. Chem., Kosmophys.* **1985**, *40*, 389–420. (c) Sharp, J. H.; Lardon, M. *J. Phys. Chem.* **1968**, *72*, 3230–3235.

(30) These studies were made by adding increasing amounts of ethanol to a diethyl ether/pentane/ethanol mixture. The electronic coupling energy was found to increase progressively with increasing mole fraction of ethanol, although the extreme values remained within 10 cm^{-1} of each other. The value used in the text refers to an ethanol mole fraction of 0.05.

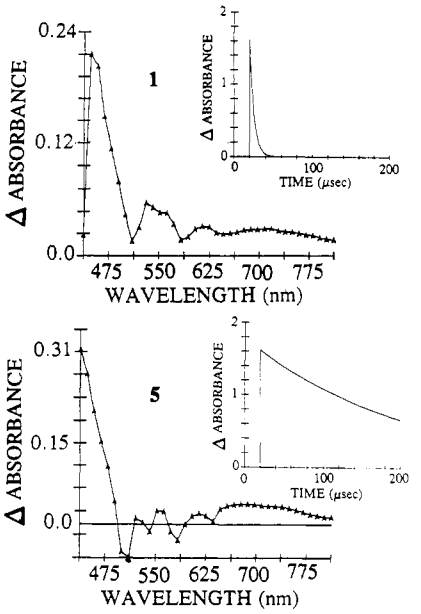

Figure 4. Triplet–triplet absorption spectra recorded in deoxygenated benzene solution for trimer **1** and unsubstituted monomer **5**. Spectra were recorded 200 ns after laser excitation at 532 nm. The inserts show decay profiles recorded at 440 nm.

The fluorescence quantum yield (Φ_f) and excited singlet state lifetime (τ_s) for the trimer **1**, as measured in benzene solution at 25 °C, were reduced by about 40% relative to the corresponding values recorded for the monomer **5**. This nonradiative quenching process does not lead to enhanced population of the excited triplet state manifold but, instead, results in an increased rate of internal conversion. There was also a substantial reduction in the triplet lifetime (τ_t) for **1** compared to the monomer, as measured in deoxygenated benzene solution (Table I). Similar quenching effects were noted[18a] for the dimer **19**. Evidently, exciton coupling

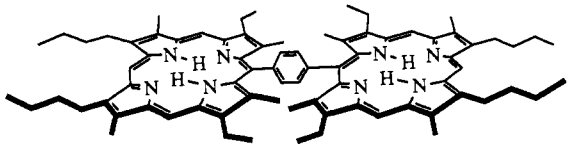

19

within the dimeric and trimeric porphyrin arrays enhances the rates of nonradiative decay pathways which couple together the excited and ground states. The increased rates may arise, in part, from a reduced energy gap due to exciton splitting of the energy levels[31] but, on the basis of the solvent polarity dependence studies, there may also be increased charge-transfer interactions in the multi-porphyrin arrays.[32] In any case, coupling between the porphyrin subunits decreases both singlet and triplet excited state lifetimes by significant amounts but the effect is not overpowering.

Further insight into the nature and degree of electronic coupling between adjacent porphyrin nuclei was sought from time-resolved transient spectroscopy. Fluorescence lifetimes were measured for the monomer **5**, dimer **19**, and trimer **1** in benzene solution using a streak camera detection system following excitation at 532 nm with a 30-ps laser pulse.[33] It was observed that the fluorescence decay profiles were independent of laser intensity, even under high-intensity conditions where several photons should be absorbed by a single molecule. In all cases, the observed fluorescence decay profiles could be analyzed satisfactorily in terms of a single exponential component. Within the 40-ps time resolution of this setup, there was no indication of a fast component in the decay records that could be attributed to singlet exciton annihilation.[34]

As a complement to the above singlet state studies, the excited triplet state lifetimes were measured for **1**, **19**, and **5** in deoxygenated benzene solution. This was done by monitoring the transient absorption change at 450 nm following excitation with a 10-ns laser pulse at 532 nm. At high laser intensity, the triplets decayed over a few μs via mixed first- and second-order kinetics, due to competition between the inherent nonradiative deactivation and intermolecular triplet–triplet annihilation.[35] At very low laser intensity, however, decay of the triplet state occurred exclusively by first-order kinetics. Actinometric measurements showed that, under high laser intensities, only a single porphyrin chromophore in the dimeric and trimeric arrays could be promoted into the triplet excited state. This effect was demonstrated clearly by the observation that, at low porphyrin concentration and high laser intensity, complete bleaching of the monomer **5** could be achieved. Under identical conditions, the maximum absorbance change attainable with the dimer **19** was exactly half that of the monomer, whereas the trimer **2** gave a maximum signal that was only one-third that of the monomer. On the basis of the above laser intensity studies, we conclude that it is possible to deposit only a single photon onto the dimeric and trimeric porphyrin arrays, at least on time scales longer than ca. 40 ps.

The most likely explanation for the above intensity-dependence studies is that energy transfer occurs between the porphyrin subunits on a time scale much faster than 40 ps. As such, it is necessary to inquire into possible mechanisms that might allow rapid energy transfer between identical porphyrin nuclei. It is well-known that the rate of transfer for both dipole–dipole (Forster)[36] and exchange (Dexter)[37] mechanisms depends on the spectral overlap between porphyrin emission and absorption transitions and can be calculated by conventional methods. For Forster-type energy transfer,[36] the overlap integral (J_F) was determined to be 1.05×10^{-14} mmol cm:[6]

$$J_F = \frac{\int F(\nu)\, \epsilon(\nu) \nu^{-4}\, d\nu}{\int F(\nu)\, d\nu} \qquad (1)$$

where $F(\nu)$ is the fluorescence intensity at wavenumber ν (in cm^{-1}) and ϵ is the molar extinction coefficient (in $cm^{-1}\ M^{-1}$), with only the Q_y absorption transition being considered. Using this value together with the photophysical data derived for the trimeric porphyrin array, the reciprocal of the energy-transfer rate constant for a photon transfer between adjacent porphyrin nuclei (τ_F) was calculated to be ca. 55 ps. This determination was made on the basis of a center-to-center separation distance (R_c) of 12.8 Å using the following expression:

$$\tau_F^{-1} = \frac{(8.8 \times 10^{-25}) K^2 \Phi_f J_F}{n^4 \tau_s R_c^6} \qquad (2)$$

Here, K is a factor which describes the mutual orientation of the porphyrin rings ($K = 2$) and n is the solvent refractive index.[36]

If the edge-to-edge separation (R_e = 5.9 Å) is used in place of R_c in the Forster-type energy-transfer calculation, τ_F is reduced

(31) Yon, Y.; Friesner, R. *J. Phys. Chem.* **1988**, *92*, 2208–2219.
(32) Tran-Thi, T. H.; Lipskier, J. F.; Maillard, P.; Momenteau, M.; Lopez-Castillo, J.-M.; Jay-Gerin, J.-P. *J. Phys. Chem.* **1992**, *96*, 1073–1082.
(33) Fluorescence was collected at 660 ± 20 nm as a function of incident laser intensity. The temporal disperser used for these studies had a time resolution of 10 ps. After deconvolution of the instrument response function, the absolute time resolution of this setup was ca. 40 ps.
(34) At the highest laser intensity used for these studies (e.g., 25 mJ), several photons should be absorbed by a single dimer or trimer molecule. The laser energy was varied progressively to <1 mJ, but the decay profile remained unaffected.
(35) Pekkarinen, L.; Linschitz, H. *J. Am. Chem. Soc.* **1960**, *82*, 2407–2411.
(36) Forster, T. *Discuss. Faraday Soc.* **1959**, *27*, 7–23.
(37) Dexter, D. L. *J. Chem. Phys.* **1953**, *21*, 836–847.

Table I. Photophysical Properties of the Various Porphyrins as Measured in Benzene Solution

porphyrin	λ_{max} (nm) Soret	λ_{max} (nm) Q	Φ_f	τ_s[a] (ns)	τ_s[b] (ps)	τ_t (μs)
1	422	508, 538, 574, 624	0.076	7.0	7 500	5.3
2	411	508, 538, 575, 625	<0.001	<0.02	18	nd
3	414	510, 541, 575, 626	<0.001	<0.02	9	nd
4	414	507, 539, 573, 624	<0.001	<0.02	12	nd
5	404	503, 537, 571, 623	0.13	11.9	12 000	200
19	420	507, 536, 574, 624	0.072	6.8	7 000	4.7
20	406	504, 538, 573, 624	<0.001	<0.02	<0.35	nd

[a] Measured by time-correlated, single-photon counting. [b] Measured by transient absorption spectroscopy.

Scheme IV. Average Time Taken for a Photon to Hop between Porphyrin Subunits as Calculated from Forster Theory Using Center-to-Center or Edge-to-Edge Separation Distances

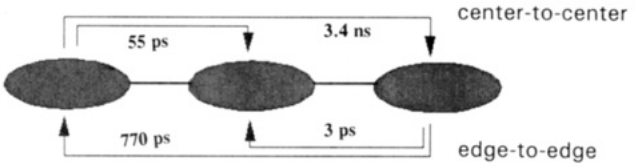

to only ca. 0.5 ps.[38] However, for closely-coupled chromophores, the R^{-6} dependence may be inappropriate and, following from the calculations of Kenkre and Knox,[39] for V = 45 cm^{-1}, we would expect to observe a dependence of $R^{-5.9}$. This would result in a value for τ_F of ca. 3 ps for adjacent porphyrins, assuming R_e = 5.9 Å. Using R_e = 19.9 Å (or R_c = 25.5 Å), the transfer time between distal porphyrin subunits in the trimeric array is calculated to be ca. 770 ps (or 3.4 ns).

For photon migration via the Dexter mechanism,[37] the overlap integral (J_D) was determined to be 5.0 × 10^{-5} cm on the basis of the following expression:

$$J_D = \frac{\int F(\nu)\,\epsilon(\nu)\,d\nu}{\int F(\nu)\,d\nu \int \epsilon(\nu)\,d\nu} \quad (3)$$

This leads to a transfer time (τ_D) between adjacent porphyrins of ca. 8 ps, assuming a coupling matrix element (H) of 45 cm^{-1} as was derived from the steady-state spectral measurements discussed above.

$$\tau_D^{-1} = \frac{4\pi^2 H^2 J_D}{h} \quad (4)$$

Allowing for the attenuation in the coupling matrix element with increased separation distance[40]

$$H = H_o^{-R/L} \quad (5)$$

where $R = R_e$ and L is the so-called Bohr radius (L = 1.5 Å), τ_D between distal porphyrins is calculated to be ca. 1 ms. Of course, this value may be decreased enormously if the interspersed porphyrin participates in a superexchange mechanism since this would reduce the magnitude of L. However, in view of the very fast rate involved, a sequential energy hopping process would appear to be a more reasonable proposition.

The above calculations indicate that, because of the close proximity of the porphyrin subunits within the linear dimeric and trimeric arrays, rapid energy transfer throughout the array should be expected. This would explain our inability to deposit more than a single photon onto the array, if indeed the transfer time is much less than 40 ps. Energy transfer between adjacent porphyrins could occur by a Dexter-type exchange mechanism (τ_D = 8 ps), or by a Forster-type dipole–dipole mechanism providing the edge-to-edge separation distance is the appropriate parameter (τ_F = 3 ps).[38] An alternative explanation involves consideration of the linear array of porphyrin subunits as being a single chromophore, but the results of various spectroscopic (e.g., ^{1}H-NMR, optical absorption and emission) studies are all consistent with but relatively weak coupling between the porphyrin subunits. Thus, this obvious possibility is ruled out and one is left with a picture wherein only rapid inter-porphyrin energy transfer is considered consistent with the experimental findings.

Scheme V. Average Time Taken for a Photon to Hop between Porphyrin Nuclei as Calculated from Dexter Theory

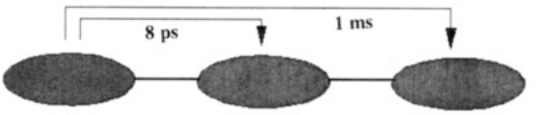

Photophysical Properties of Quinone-Substituted Porphyrin Arrays. Steady-state fluorescence from the quinone-bearing dimeric (**4**) and trimeric (**2**) porphyrins was reduced to very low levels (i.e., Φ_f < 0.001). Similarly, time-resolved fluorescence studies employing single-photon counting detection methods could not resolve emission from these porphyrinic chromophores. The excited singlet state of the porphyrin subunits could be detected readily, however, by transient absorption spectroscopy following excitation of **2** or **4** in benzene solution with a 0.5-ps laser pulse at 586 nm. The observed differential absorption spectral features of the quinone-substituted trimer **2** were similar, if not identical, to those recorded for the quinone-free monomer **5**, dimer **19**, and trimer **1** (Figure 5). However, whereas the excited singlet states of the quinone-free compounds decayed over many nanoseconds to form the corresponding triplet excited states, deactivation of the excited singlet states of **2** and **4** resulted in rapid restoration of the ground state. From these studies, excited singlet state lifetimes of ca. 18 ± 6 (see later) and 12 ± 3 ps, respectively, were derived for compounds **2** and **4** (Figure 6, Table I). Triplet-state formation was not observed for these latter compounds, and the spectral records gave no indication of intermediate formation of redox products. In particular, the putative formation of porphyrin π-radical cation (and quinone π-radical anion) states could be rigorously excluded as species surviving for times in excess of the porphyrin excited singlet states.

The above results have to be compared to earlier studies carried out with the quinone-bearing porphyrin monomer **20**.[18b] Here,

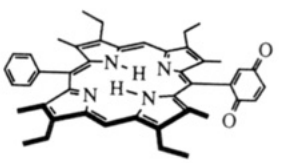

20

(38) The Forster equation uses the center-to-center separation distance. However, to our knowledge, there have been no experimental tests to determine whether center-to-center or edge-to-edge separations are the more appropriate distance parameters to use when describing Forster-type energy transfer in rigidly-linked intramolecular systems. Therefore, we have included both calculations. Still, our belief is that those based on the use of center-to-center separations are likely to be the more reliable.

(39) Kenkre, V. M.; Knox, R. S. *Phys. Rev. Lett.* **1974**, *33*, 803–806.

(40) Oevering, H.; Verhoeven, J. W.; Paddon-Row, M. N.; Cotsaris, E. *Chem. Phys. Lett.* **1988**, *143*, 488–495.

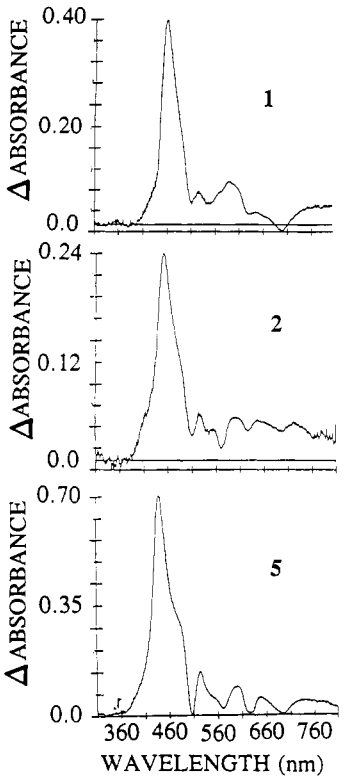

Figure 5. Transient absorption spectra recorded in benzene solution for trimer **1**, monoquinone-substituted trimer **2**, and the unsubstituted monomer **5**. Spectra were recorded 2 ps after excitation with a 0.5-ps laser flash at 586 nm.

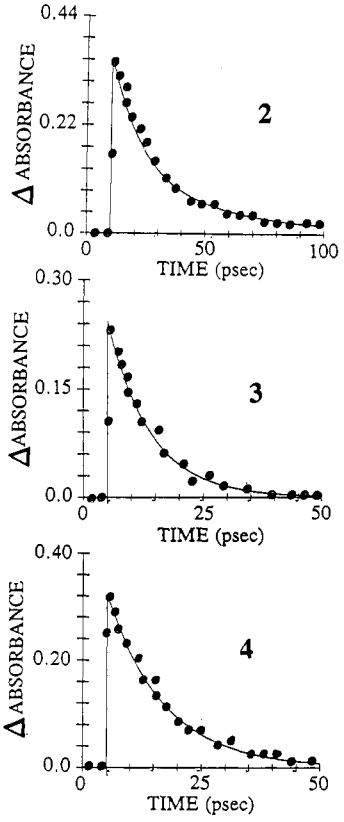

Figure 6. Decay profiles recorded at 450 nm following excitation with a 0.5-ps laser pulse at 586 nm for monoquinone-substituted dimer **4**, monoquinone-substituted trimer **2**, and diquinone-substituted trimer **3**.

it was established by transient absorption spectroscopy that the excited singlet state lifetime of the porphyrin subunit was reduced to <350 fs, compared to 11.9 ns observed for the quinone-free monomer **5**.[18b] The transient absorption spectral features observed after decay of the excited singlet state could be assigned to the porphyrin π-radical cation, as formed by electron transfer from porphyrin to appended quinone. Decay of the porphyrin π-radical cation occurred by first-order kinetics with a lifetime of 5.9 ± 0.5 ps.

Following from these experiments,[18b] and the many studies made with structurally-related porphyrin–quinone systems,[10-18] it seems most likely that the efficient excited singlet state quenching observed for **2** and **4** is also due to photoinduced electron transfer from porphyrin to appended quinone. The reaction exergonicity for photoinduced charge separation (ΔG° = –0.69 eV) and subsequent charge recombination (ΔG° = –1.27 eV) remains unaffected by the number of porphyrin subunits in the linear array,[18] such that electron transfer is thermodynamically favorable in each case. Our failure to detect intermediate formation of the porphyrin π-radical cation for compounds **2** and **4** is presumed to be because its lifetime is shorter than that of the observed excited singlet state. Indeed, on the basis of the previously determined kinetic data for the quinone-bearing monomer **19**,[18b] we conclude that the excited singlet states observed here for **2** and **4** are associated with porphyrin subunits which are not bound directly to the terminal quinone. The excited singlet state associated with the proximal porphyrin is expected to be too short-lived (τ_s < 350 fs) to be resolved by our instrument (time resolution ca. 800 fs). Thus, the fact that no porphyrin π-radical cation state is observed is not surprising.

Support for the above conclusion was obtained by performing actinometric laser flash photolysis studies employing a 0.5-ps laser pulse at 586 nm and using the monomer **5** as a reference. The initial transient absorbance at 450 nm, as measured by computer extrapolation to the center of the laser pulse, was measured at several laser intensities for compounds **5**, **2**, and **4**, under conditions where the transient absorption increased linearly with increasing laser intensity. Relative to the values determined for **5** at any given laser intensity, the initial absorbances for the trimer **2** and the dimer **4**, respectively, were 0.70 and 0.55. On the basis of identical extinction coefficients and assuming that the proximal porphyrin makes no contribution to the transient absorption, we would expect to observe relative initial absorbances of 0.67 and 0.50, respectively, for **2** and **4**. Studies carried out with the trimeric porphyrin bearing two terminal quinones (**3**) indicated a relative initial absorbance of 0.42, compared to an expected value of 0.33.

The τ_s values observed for **2** and **4** (Table I) may refer either to the rate of long-distance electron transfer to the terminal quinone in the absence of energy transfer or to the time that it takes a photon absorbed by a distant porphyrin to reach the proximal porphyrin. In the absence of superexchange, the rate of long-distance electron transfer (k_{et}) can be expressed in the form

$$k_{et} = A \exp[-\beta R_e] \qquad (6)$$

where the attenuation factor β is assigned[41] a value of 0.4 Å^{-1}. Using the single datum point obtained for **19** as a reference ($A = 7 \times 10^{12}$ s^{-1}), k_{et} values of 9×10^9 and 6×10^7 s^{-1} were calculated for photoinduced electron transfer across one and two porphyrin nuclei, respectively. These values require porphyrin excited singlet state lifetimes much longer than those observed for **2** and **4**. Thus,

(41) The attenuation factor (β = 0.4 Å^{-1}) is assumed to have the same value as that determined experimentally for aromatic spacer groups separating bis-phorphyrins.[41b,c] It has been argued by Helms *et al.*[41c] that the orthogonicity of the spacer group needs to be considered, but this finding is not apparent in the data reported by Osuka *et al.*[41b] Thus, the choice of β = 0.4 Å^{-1} seems appropriate in the present instance. (b) Osuka, A.; Maruyama, H.; Mataga, N.; Asaki, T.; Yamazaki, I.; Tamdi, H. *J. Am. Chem. Soc.* **1990**, *112*, 4958–4959. (c) Helms, A.; Heiler, D.; McLendon, G. *J. Am. Chem. Soc.* **1992**, *114*, 6227–6238.

Scheme VI. Singlet Excited State Lifetimes Expected for Each Porphyrin Subunit in the Event of Electron Transfer to the Terminal Quinone but without Photon Migration

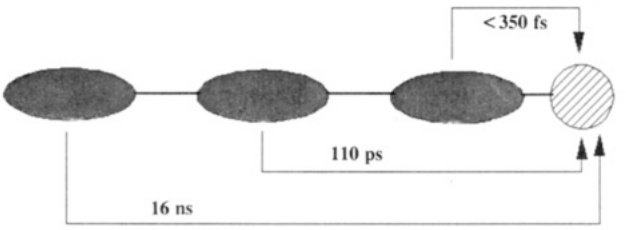

Scheme VII. Average Time That a Photon Spends on a Particular Porphyrin Subunit in the Event of Electron Transfer to the Terminal Quinone and Allowing for Incoherent Photon Migration

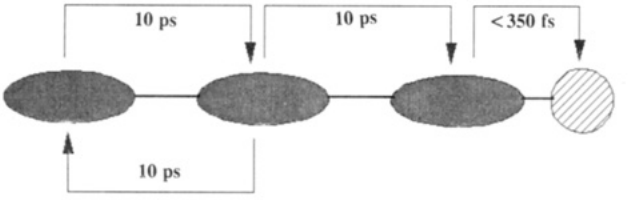

this explanation, which is summarized in Scheme VI, is inconsistent with the experimental data.

In light of the above analysis, the measured τ_s values for **2**, **3**, and **4** are believed to refer to the average time taken for an absorbed photon to reach to the proximal porphyrin. For both **3** (τ_s = 9 ± 3 ps) and **4** (τ_s = 12 ± 3 ps), only a single transfer step is possible if the rate of trapping (τ > 350 fs) greatly exceeds the rate of transfer. The time required for a photon to transfer between adjacent porphyrins within a linear array, therefore, is ca. 10 ps. This value is consistent with the laser intensity dependence studies carried out with the quinone-free porphyrin arrays and is in exact accord with the value calculated for transfer via the Dexter mechanism (τ_D = 8 ps). This latter agreement is certainly fortuitous. The situation is more complicated for **2** since the multiple energy-transfer steps may occur. For this compound, the excited singlet state decay profiles did not give good fits to a single exponential decay law and the quoted τ_s value (τ_s = 18 ± 6 ps) is an approximation. The decay data, however, could be readily analyzed in terms of an unsymmetrical distribution of lifetimes centered around a mean value of 15 ps. Again, this is entirely consistent with an incoherent energy-transfer mechanism, such as that shown in Scheme VII.

Concluding Remarks. The linear porphyrin arrays described here differ from most other photosynthetic model systems in that they demonstrate rapid energy transfer between identical pigments prior to photon trapping at a redox-active site. The time needed for a photon to transfer between porphyrins separated by an edge-to-edge distance of 5.9 Å is ca. 10 ps. This transfer time is significantly slower than those reported for photosynthetic bacterial light harvesting arrays[42,43] where the coupling energies are notably higher.[44] It is interesting to record that calculations of the transfer time for the bacterial systems, which are based on Forster's weak coupling limit, lead to energy-transfer times at least an order of magnitude longer than those measured by femtosecond spectroscopy.[43] We cannot assign the energy-transfer process to a particular (Dexter or Forster) mechanism because the calculated rates are too similar and both are close to the observed rate.

By extending the basic synthetic strategy described herein, it should be possible to construct supramolecular arrays containing five or, perhaps, even seven porphyrin subunits. These larger arrays would permit us to model the overall energy-transfer process by Monte Carlo methods. We expect to explore such systems in the near future, using fluorescence upconversion techniques to provide more precise data concerning the porphyrin excited singlet state lifetimes. In any case, these new systems are expected to act as improved models for the light-harvesting (antenna) portion of the natural RC. Synthetic work directed toward the production of such elaborate systems, therefore, is currently underway in our laboratories.

Experimental Section

General Information. Melting points were measured on a Mel-temp apparatus and are uncorrected. All solvents and chemicals were of reagent grade quality, purchased commercially, and used without further purification except as noted below. CH_2Cl_2 when used as a solvent was heated at reflux with and distilled from CaH_2. Column chromatography on silica gel was performed on Merck type 60 (230–400 mesh) silica gel. Thin-layer chromatography (TLC) was performed on commercially prepared silica gel plates purchased from Analtech, Inc., or Whatman International, Inc.

Electronic spectra were recorded on a Beckman DU-7 spectrophotometer. Proton and ^{13}C NMR spectra were obtained in $CDCl_3$ or CD_3CN with either Me_4Si or the solvent as an internal standard. Proton spectra were recorded on a General Electric QE-300 (300 MHz) spectrometer. The peak assignments given were made on the basis of integrations and spectral comparisons with similar compounds. Carbon spectra were measured at 75 or 125 MHz with use of either a General Electric QE-300 or Nicolet NT-500 spectrometer, respectively. Low-resolution mass spectra were measured with either a Finnigan-MAT 4023 or Bell and Howell 21-491 instrument. Fast atom bombardment mass spectra (FAB MS) were determined with a Finnigan-MAT TSQ-70 instrument and 3-nitrobenzyl alcohol matrix. High-resolution mass spectra were obtained with a Bell and Howell 21-110B instrument. Elemental analyses were performed by Atlantic Microlabs, Inc., Norcross, GA.

Luminescence spectra were recorded with a Perkin-Elmer LS5 spectrofluorimeter and are corrected for wavelength responses of the detector. Singlet excited state lifetimes were measured by time-correlated, single photon counting using a mode-locked Nd-YAG laser (Antares 76S) synchronously pumping a cavity-dumped Rhodamine 6G dye laser (Spectra Physics 375B/244). Glass cutoff filters were used to isolate fluorescence from scattered laser light. A Hamamatsu microchannel plate was used to detect emitted photons, for which the instrument response function had a fwhm of 50 ± 10 ps. Data analyses were made according to O'Connor and Phillips[45] using computer deconvolution to minimize reduced χ^2 parameters. All solutions for fluorescence studies were optically dilute (optical density ca. 0.08) and air equilibrated.

Flash photolysis studies were made with a frequency-doubled, mode-locked Quantel YG402 Nd-YAG laser.[46] Solutions were adjusted to possess absorbances of ca. 0.6 at the excitation wavelength of 532 nm, and 300 laser shots were averaged for each measurement. Residual 1064-nm output from the laser was focused into 1:1 D_3PO_4/D_2O to produce a white light continuum for use as the analyzing beam. Variable delay times in the range 0–6 ns were selected in a random sequence, and transient spectra were recorded with an Instruments SA UFS200 spectrograph interfaced to a Tracor Northern 6200 MCA and a microcomputer. Kinetic analyses were made by overlaying about 30 individual spectra and fitting data at selected wavelengths using computer-based nonlinear, least-squares iterative procedures.

Improved time resolution was achieved using a frequency-doubled, mode-locked Antares 76S Nd-YAG laser to pump a Coherent 700 dual jet (Rhodamine 6G) dye laser operated at 76 MHz. A Quantel model RGA67-10 regenerative amplifier, a Quantel model PTA-60 dye laser, and a Continuum SPA1 autocorrelator was used to obtain 3-mJ pulses at 586 nm having a fwhm of ca. 500 fs. The spectrometer was run at

(42) Breton, J.; Martin, J.-L.; Migus, A.; Antonetti, A.; Orszag, A. *Proc. Natl. Acad. Sci. U.S.A.* **1986**, *83*, 5121–5125.
(43) Jean, J. M.; Chan, C.-K.; Fleming, G. R. *Isr. J. Chem.* **1988**, *28*, 169–175.
(44) Knapp, E. W.; Fischer, S. F.; Zinth, W.; Sander, M.; Kaiser, W.; Deisenhofer, J.; Michel, H. *Proc. Natl. Acad. Sci. U.S.A.* **1985**, *82*, 8463–8567.
(45) O'Connor, D. V.; Phillips, D. *Time Resolved Single Photon Counting*; Academic: London, 1984.
(46) Atherton, S. J.; Hubig, S. M.; Callen, T. J.; Duncanson, J. A.; Snowden, P. T.; Rodgers, M. A. J. *J. Phys. Chem.* **1987**, *91*, 3137–3140.

a frequency of 10 Hz, and data were acquired through a Princeton dual diode array spectrograph interfaced to a microcomputer. The detection setup and optical delay line were similar to those used for the 30-ps pulse width experiments except that the exciting and analyzing beams were almost collinear and a polarizing scrambler was inserted into the analyzing beam pathway. Again, kinetic analyses were made by overlaying spectra collected at about 50 different delay times.

Bis(5-(ethoxycarbonyl)-4-ethyl-3-methyl-2-pyrryl)(4-(hydroxymethyl)phenyl)methane (8). A 250-mL round-bottomed flask equipped with a reflux condensor was charged with **6** (9.02 g, 43.1 mmol), **7** (15.96 g, 88.2 mmol), and 175 mL of absolute ethanol. A few drops of concentrated HCl were added, and the solution was heated at reflux for 8 h with magnetic stirring under nitrogen gas. At the end of this time, TLC (silica gel, 20% EtOAc/hexane eluent) indicated the absence of starting material with the complete formation of what was presumed to be the desired product. The solvent was removed *in vacuo* by rotary evaporation, and the red oil was loaded onto a silica gel column. Elution with 20% EtOAc/hexane yielded the product as a pale yellow oil. Drying under high vacuum gave the dipyrrylmethane **8** as a pale yellow crystalline material (15.5 g, 32.4 mmol) in 75% yield, mp 128–130 °C. ^{1}H NMR (300 MHz, $CDCl_3$): δ 1.10 (6H, t (J = 7.4 Hz), CH_2CH_3), 1.31 (6H, t (J = 7.0 Hz), $CO_2CH_2CH_3$), 1.79 (6H, s, CH_3), 2.72 (4H, q (J = 7.5 Hz), CH_2CH_3), 4.25 (4H, q (J = 7.1 Hz), $CO_2CH_2CH_3$), 4.70 (2H, d (J = 4.3 Hz), CH_2OH), 5.48 (1H, s, CH_3), 7.33 (4H, dd, aromatic), 8.24 (2H, s, NH) ppm. ^{13}C NMR (300 MHz, $CDCl_3$): δ 8.6, 14.4, 15.1, 18.4, 40.8, 59.8, 64.8, 117.1, 117.2, 127.6, 128.4, 131.7, 134.2, 138.4, 140.1, 161.6 ppm. Mass spectrum (CI, 70 eV): m/z (relative intensity, %) 480 (M^+, 100), 481 (M^+ + 1, 26). Exact mass for $C_{28}H_{36}N_2O_5$: calculated 480.2624, found 480.2621.

Bis(4-ethyl-3-methyl-2-pyrryl)(4-(hydroxymethyl)phenyl)methane (9). A 500-mL round-bottomed flask equipped with a side arm and a reflux condensor was charged with the dipyrrylmethane **8** (15.5 g, 0.032 mol), 300 mL of 95% ethanol, and 20.2 g of sodium hydroxide pellets. The reaction mixture was heated at reflux for 2 h under the flow of nitrogen gas. At this time, TLC (silica gel, 20% EtOAc/hexanes eluent) indicated the absence of starting material and the presence of a deep red, slow-moving component which was presumed to be the sodium salt of the hydrolyzed dicarboxylate dianion. The condensor was removed, and the ethanol was evaporated under the flow of nitrogen. When the reaction volume had reached 50 mL, ethylene glycol (300 mL) was added and the system brought to 185 °C with a heating mantel. After the temperature had reached 185 °C, the condensor was replaced and the reaction stirred for an additional 30 min. Heating was discontinued, and the tan solution cooled to room temperature. Upon cooling of the solution, first at room temperature and then in the freezer, the product was obtained as a tan precipitate. This precipitate was filtered off, washed with H_2O, and dried to afford the pure α-free dipyrrylmethane **9** (11.62 g, 0.030 mol) in 94.8% yield, mp 149–151 °C. ^{1}H NMR (300 MHz, $CDCl_3$): δ 1.17 (6H, t (J = 7.4Hz), CH_2CH_3), 1.65 (1H, br s, OH), 1.79 (6H, s, CH_3), 2.42 (4H, q (J = 7.4 Hz), CH_2CH_3), 4.68 (2H, s, CH_2OH), 5.49 (1H, s, CH_3), 7.21 (4H, dd, phenyl-H) ppm. ^{13}C NMR (300 MHz, $CDCl_3$): δ 8.87, 14.11, 18.67, 40.64, 64.99, 111.96, 113.54, 125.99, 127.36, 127.50, 128.49, 138.97, 141.10 ppm. Mass spectrum (EI, 70 eV): m/z (relative intensity, %) 336 (M^+, 93), 337 (M^+ + 1, 51).

5-(4′-(Hydroxymethyl)phenyl)-13,17-dibutyl-2,8-diethyl-3,7,12,18-tetramethylporphyrin (12). A 500-mL Erlenmeyer flask was charged with **10**[18a] (509 mg, 1.48 mmol), **9** (500 mg, 1.48 mmol), and 160 mL of THF:MeOH (2:1). The reaction mixture was bubbled with dry N_2 and covered with foil, and then 0.5 mL of $HClO_4$(aq) was added with stirring. The reaction was allowed to stir in the dark for 12 h, after which *o*-chloranil (0.6 g) was added and the reaction stirred for an additional 12 h. The reaction mixture was poured into brine and extracted several times with CH_2Cl_2. The organic layers were combined, washed with K_2CO_3(aq) and H_2O, and dried over Na_2SO_4, and the solvent was removed on a rotary evaporator to give a dark solid. After chromatography on silica gel (2% MeOH/$CHCl_3$ eluent), the product **12** was isolated (662 mg, 1.03 mmol) in 69.6% yield. UV–vis: λ_{max} 404, 503, 536, 569, 622 nm. ^{1}H NMR (300 MHz, $CDCl_3$): δ 1.26 (6H, t (J = 7.2 Hz), 13,17-$CH_2CH_2CH_2CH_3$), 1.85 (6H, t (J = 6.8 Hz), 2,8-CH_2CH_3), 1.95 (4H, m, 13,17-$CH_2CH_2CH_2CH_3$), 2.33 (4H, quintet (J = 7.0 Hz), 13,17-$CH_2CH_2CH_2CH_3$), 2.46 (6H, s, 3,7-CH_3), 3.62 (6H, s, 12,18-CH_3), 3.96 (4H, t (J = 7.2 Hz), 13,17-$CH_2CH_2CH_2CH_3$), 4.03 (4H, t (J = 6.6 Hz), 2,8-CH_2CH_3), 4.94 (2H, br s, CH_2OH), 7.90 (4H, dd, 2′,3′-H), 9.88 (1H, s, 15-H), 10.19 (2H, s, 10,20-H) ppm. ^{13}C NMR (300 MHz, $CDCl_3$): δ 11.6, 14.1, 14.4, 17.3, 19.8, 23.1, 26.0, 35.1, 64.8, 96.1, 96.6, 118.7, 126.0, 133.4, 135.9, 136.6, 140.7, 140.9, 142.8, 143.9, 144.1, 146.2 ppm. Mass spectrum (FAB, 70 eV): m/z (relative intensity, %) 641 (M^+ + 1, 100), 642 (M^+ + 2, 48), 643 (M^+ + 3, 12). Exact mass for $C_{43}H_{53}N_4O$: calcd 641.4219, obsd 641.4217.

5-(4′-Formylphenyl)-13,17-dibutyl-2,8-diethyl-3,7,12,18-tetramethylporphyrin (14). A 250-mL round-bottomed flask was charged with **12** (662 mg, 1.03 mmol), 100 mL of freshly distilled CH_2Cl_2, and PDC (1.01 g, 2.7 mmol). The reaction mixture was allowed to stir for 3 h under nitrogen, at which time TLC (2% MeOH/$CHCl_3$ eluent) indicated the complete conversion of starting material into product. After complete conversion of starting material, the reaction mixture was poured into brine and extracted several times with CH_2Cl_2. The organic layers were combined, washed several times with H_2O, and dried over Na_2SO_4, and the solvent was removed on a rotary evaporator. The product was purified by chromatography on silica gel (2% MeOH/$CHCl_3$ eluent, $R_f \sim 0.8$) and recrystallized from $CHCl_3$/hexanes to give **14** as bright violet crystals (472 mg, 0.74 mmol) in 74% yield. UV–vis ($CHCl_3$): λ_{max} 405, 503, 537, 571, 623 nm. ^{1}H NMR (300 MHz, $CDCl_3$): δ –3.21 (2H, br s, NH), 1.21 (6H, t (J = 6.9 Hz), $CH_2CH_2CH_2CH_3$), 1.78 (6H, t (J = 7.5 Hz), CH_2CH_3), 2.33 (4H, m, $CH_2CH_2CH_2CH_3$), 2.40 (4H, m, $CH_2CH_2CH_2CH_3$), 2.41 (6H, s, 3,7-CH_3), 3.66 (6H, s, 12,18-CH_3), 4.03 (8H, m, CH_2CH_3 and $CH_2CH_2CH_2CH_3$), 8.18 (4H, dd (J = 5.0 Hz), Ar-H), 9.95 (1H, s, 15-H), 10.21 (2H, 2, 10, 20-H), 10.36 (1H, s, CHO) ppm. ^{13}C NMR (300 MHz, $CDCl_3$): δ 11.75, 14.23, 14.79, 11.57, 19.90, 23.11, 26.17, 35.24, 95.98, 96.63, 117.05, 128.69, 133.89, 135.35, 136.13, 136.22, 140.46, 141.86, 143.25, 143.99, 144.54, 145.96, 149.58, 192.39 ppm. Mass spectrum (FAB, 70 eV): m/z (relative intensity, %) 640 (M^+, 100), 641 (M^+ + 1, 23), 642 (M^+ + 2, 8). Exact mass for $C_{43}H_{51}N_4O$: calcd 639.4062, obsd 639.4055. Anal. Calcd for $C_{43}H_{50}N_4$: C, 80.83; H, 7.89; N, 8.77. Found: C, 80.74; H, 7.86; N, 8.78.

5-(2′,5′-Dimethoxyphenyl)-15-(4″-(hydroxymethyl)phenyl)-2,8,12,18-tetraethyl-3,7,13,17-tetramethylporphyrin (13). A 500-mL round-bottomed flask fitted with a nitrogen inlet was charged with **11**[18a] (1.01 g, 2.4 mmol), **9** (0.81 g, 2.4 mmol), and 240 mL of THF:MeOH (2:1). The flask was shielded from ambient lighting, and the solution was stirred under nitrogen for 10 min. Perchloric acid (70%, 0.4 mL) was added with stirring, and the reaction was allowed to proceed for 12 h. *o*-Chloranil (0.7 g) was added and the reaction stirred for an additional 3 h. The reaction mixture was poured into brine and extracted several times with $CHCl_3$. The organic fraction was washed several times with water and dried over Na_2SO_4. The drying agent was filtered off, and the solvent removed *in vacuo*. The porphyrin product was purified by chromatography on silica gel (2% MeOH/$CHCl_3$ eluent, $R_f \sim 0.3$) and recrystallization from $CHCl_3$/hexanes to give **13** as a pale purple solid (750 mg, 1.04 mmol) in 51% yield. UV–vis ($CHCl_3$): λ_{max} 410, 507, 540, 574, 625 nm. ^{1}H NMR (300 MHz, $CDCl_3$): δ –2.39 (2H, s, NH), 1.74 (6H, t (J = 7.5 Hz), CH_2CH_3), 1.77 (6H, t (J = 7.5 Hz), CH_2CH_3), 2.49 (6 H, s, CH_3), 2.63 (6H, s, CH_3), 3.69 (3H, s, OCH_3), 3.87 (3H, s, OCH_3), 4.03 (8H, m, CH_2CH_3), 5.09 (2H, s, CH_2OH), 7.90 (4H, dd, Ar-H), 8.06 (3H, m, Ar-H), 10.21 (2H, s, 10,20-H) ppm. ^{13}C NMR (300 MHz, $CDCl_3$): δ 13.0, 13.6, 16.4, 16.5, 19.6, 56.1, 64.7, 77.1, 97.1, 112.1, 114.8, 116.9, 117.7, 119.5, 120.5, 121.2, 126.4, 126.6, 128.4, 134.5, 134.8, 136.2, 136.4, 138.1, 139.8, 140.6, 140.9, 142.3, 142.5, 144.0, 144.7, 152.6, 154.3 ppm. Mass spectrum (FAB, 70 eV): m/z (relative intensity, %) 720 (M^+, 83), 721 (M^+ + 1, 100), 722 (M^+ + 2, 44), 723 (M^+ + 3, 12). Exact mass for $C_{47}H_{53}N_4O_3$: calcd 721.4117, obsd 721.4114.

5-(4′-Formylphenyl)-15-(2″,5″-dimethoxyphenyl)-2,8,12,18-tetraethyl-3,7,13,17-tetramethylporphyrin (15). A 250-mL round-bottomed flask was charged with **13** (0.246 g, 0.341 mmol) and 150 mL of freshly distilled CH_2Cl_2 under an atmosphere of nitrogen. Pyridinium dichromate (0.40 g, 1.06 mmol) was added, and the reaction was allowed to stir under nitrogen until TLC (2% MeOH/$CHCl_3$ eluent) indicated the complete absence of starting material. The reaction contents were poured into brine and extracted with CH_2Cl_2. The organic solution was washed several times with water and dried over Na_2SO_4, and the solvent removed *in vacuo*. The porphyrin benzaldehyde was purified first by chromatography (silica gel, 2% MeOH/$CHCl_3$ eluent, $R_f \sim 0.8$) and then recrystallized ($CHCl_3$/hexanes) to give **15** as violet crystals (216 mg, 0.300 mmol) in 88% yield. UV–vis: λ_{max} 410, 507, 540, 574, 625 nm. ^{1}H NMR (300 MHz, $CDCl_3$): δ –2.35 (2H, br s, NH), 1.79 (6H, t (J = 7.7 Hz), CH_2CH_3), 1.82 (6H, t (J = 7.7 Hz), CH_2CH_3), 2.45 (6H, s, CH_3), 2.65 (6H, s, CH_3), 3.69 (3H, s, OCH_3), 3.89 (3H, s, OCH_3), 4.05 (4H, q (J = 7.5 Hz), CH_2CH_3), 4.08 (4H, q (J = 7.1 Hz), CH_2CH_3), 7.35 (3H, m, 3″,4″,6″-H), 8.22 (4H, s, 2′,3′-H), 10.26 (1H, s, CHO), 10.36 (2H, s, 10,20-H) ppm. ^{13}C NMR (300 MHz, $CDCl_3$): δ 13.63, 14.63, 17.80 (2C), 19.94 (2C), 56.07, 96.61, 106.28, 111.87, 113.81, 115.10, 120.31, 128.76, 129.28, 131.39, 131.64, 133.81, 134.93, 135.88, 136.10, 140.96,

141.25, 144.06, 144.61, 144.84, 145.55, 153.67, 153.96, 192.43 ppm. Mass spectrum (FAB, 70 eV): *m/z* (relative intensity, %) 718 (M^+, 100), 719 ($M^+ + 1$, 93.91), 720 ($M^+ + 2$, 60.90), 721 ($M^+ + 3$, 17.36). Exact mass for $C_{47}H_{51}N_4O_3$: calculated 719.3961, found 719.3943.

5,15-Bis(4′-(5″-(13‴,17‴-dibutyl-2‴,8‴-diethyl-3‴,7‴,12‴,18‴-tetramethylporphyrinyl))phenyl)-2,8,12,18-tetrabutyl-3,7,13,17-tetramethylporphyrin (1). A 50-mL, three-necked, round-bottomed flask equipped with septum port, reflux condensor, and argon inlet was charged with **14** (152 mg, 0.2377 mmol, 10^{-2} M) and 23.7 mL of freshly distilled CH_2Cl_2. The solution was bubbled with argon gas for 15 min. To this solution were added **16**[22] (67.9 mg, 0.2377 mmol, 10^{-2} M) and trifluoroacetic acid (18.2 μL), and the reaction was stirred in the dark, under argon, for 4 h. *o*-Chloranil (84 mg, 0.3404 mmol, 1.5×10^{-2} M) was added, and the reaction vessel placed in a preheated 50 °C bath for 8 h. The solvent was then removed *in vacuo*. Following chromatography on silica gel (2% MeOH/$CHCl_3$ eluent) and recrystallization from $CHCl_3/CH_3OH$, pure **1** (170 mg, 0.098 mmol) was isolated as a purple solid in 81.6% yield. UV–vis ($CHCl_3$): λ_{max} 422, 508, 538, 574, 624 nm. ^{1}H NMR (300 MHz, $CDCl_3$): δ −2.97 (2H, br s, N″*H*), −2.77 (2H, br s, N‴*H*), −1.44 (2H, br s, N*H*), 1.07 (12H, t (J = 7.36 Hz), 13‴,17‴-$CH_2CH_2CH_2CH_3$), 1.28 (12H, t (J = 7.4 Hz), 2,8,12,18-$CH_2CH_2CH_2CH_3$), 1.67 (8H, sextet (J = 7.3 Hz), 13‴,17‴-$CH_2CH_2CH_2CH_3$), 1.93 (12H, t (J = 7.5 Hz), 2″,8″-CH_2CH_3), 1.96 (8H, sextet (J = 7.5 Hz), 2,8,12,18-$CH_2CH_2CH_2CH_3$), 2.17 (8H, quintet (J = 7.4 Hz), 13‴,17‴-$CH_2CH_2CH_2CH_3$), 2.37 (8H, quintet (J = 6.6 Hz), 2,8,12,18-$CH_2CH_2CH_2CH_3$), 2.78 (12H, s, 3,7,13,17-CH_3), 2.80 (12H, 3‴,7‴-CH_3), 3.67 (12H, s, 12‴,18‴-CH_3), 3.75 (8H, t (J = 7.4 Hz), 13‴,17‴-$CH_2CH_2CH_2CH_3$), 4.20–4.22 (16H, m, 2,8,12,18-$CH_2CH_2CH_2CH_3$ and 2″,8″-CH_2CH_3), 7.61 (8H, s, 2′,3′-*H*), 9.58 (1H, s, 15″-*H*), 10.29 (4H, s, 10‴,20‴-*H*), 10.48 (2H, s, 10,-20-*H*) ppm. ^{13}C NMR (300 MHz, $CDCl_3$): δ 11.7, 14.0, 14.4, 16.9, 17.0, 17.7, 20.0, 22.9, 23.6, 25.9, 26.8, 35.1, 35.7, 95.4, 96.4, 97.1, 117.7, 118.6, 132.4, 132.7, 135.4, 135.6, 135.8, 140.0, 141.0, 141.1, 141.5, 141.7, 142.8, 143.5, 143.8, 144.7, 145.7, 145.8 ppm. Mass spectrum (FAB, 70 eV) *m/z* (relative intensity, %) 1808 (M^+, 70), 1809 ($M^+ + 1$, 100), 1810 ($M^+ + 2$, 73), 1811 ($M^+ + 3$, 34), 1812 ($M^+ + 4$, 12). Exact mass for $C_{124}H_{151}N_{12}$: calcd 1808.2184, obsd 1808.2129.

5,15-Bis(4′-(15″-(2‴,5‴-dimethoxyphenyl)-2‴,8‴,12‴,18‴-tetraethyl-3‴,7‴,13‴,17‴-tetramethylporphyrinyl)phenyl)-2,8,12,18-tetrabutyl-3,7,-13,17-tetramethylporphyrin (17). A 50-mL three-necked, round-bottomed flask equipped with argon inlet, reflux condensor, and septum port was charged with **15** (212 mg, 0.295 mmol, 10^{-2} M), **16**[18a] (85 mg, 0.297 mmol, 10^{-2} M), and 30 mL of CH_2Cl_2. The solution was then bubbled with argon for 15 min. Trifluoroacetic acid (22.7 μL) was added *via* syringe, and the reaction was allowed to stir in the dark for 3.5 h under a blanket of argon. *o*-Chloranil (109 mg, 0.449 mmol) was added, and the reaction was placed in a preheated 40 °C oil bath and allowed to stir for an additional 3 h. At this time, TLC (2% MeOH/$CHCl_3$) indicated the complete absence of the starting porphyrin aldehyde **15** and the appearance of a new porphyrin-like spot at lower R_f. The solvent was removed *in vacuo*, and the trimeric porphyrin **17** was purified by chromatography on silica gel (2% MeOH/$CHCl_3$ eluent) and recrystallization from $CHCl_3$/hexanes to give the desired product (201 mg, 0.0892 mmol) in 60.4% yield. UV–vis ($CHCl_3$): λ_{max} 414, 510, 541, 575, 626 nm. ^{1}H NMR (300 MHz, $CDCl_3$): δ −1.84 (3H, br s, N*H*), −1.47 (3H, br s, N*H*), 1.24 (12H, t (J = 7.3 Hz), 3,7,13,17-$CH_2CH_2CH_2CH_3$), 1.86 (8H, m, 2,8,12,18-$CH_2CH_2CH_2CH_3$), 1.93 (12H, t (J = 7.59Hz), 12″,18″-CH_2CH_3), 1.96 (12H, t (J = 7.3 Hz), 2″,8″-CH_2CH_3), 2.37 (8H, m, 2,8,12,18-$CH_2CH_2CH_2CH_3$), 2.68 (12H, s, 13″,-17″-CH_3), 3.22 (12H, s, 3,7,13,17-CH_3), 3.23 (12H, s, 3″,7″-CH_3), 3.73 (6H, s, OCH_3), 3.89 (6H, s, OCH_3), 4.11 (16H, m, 12″,18″-CH_2CH_3 and 2″,8″-CH_2CH_3), 4.21 (8H, m, 2,8,12,18-$CH_2CH_2CH_2CH_3$), 7.29 (6H, m, 2‴,4‴,6‴-*H*), 8.17 (8H, dd, 2′,3′-*H*), 10.34 (4H, s, 10″,20″-*H*), 10.47 (2H, s, 10,20-*H*) ppm. ^{13}C NMR (500 MHz, $CDCl_3$): δ 13.64, 14.41, 17.33, 17.45, 17.69, 17.78, 20.02, 20.16, 23.61, 26.82, 35.72, 56.05, 56.12, 96.61, 97.34, 111.89, 113.68, 115.12, 117.89, 118.06, 120.25, 131.66, 133.30, 133.41, 133.47, 135.38, 135.74, 135.98, 140.77, 141.06, 141.22, 143.37, 144.51, 144.56, 144.67, 145.55, 145.66, 146.04, 153.70, 153.93 ppm. FAB MS (70 eV, NBA): *m/z* (relative intensity, %) 1967 (M^+, 100), 1968 ($M^+ + 1$, 64), 1969 ($M^+ + 2$, 43), 1970 ($M^+ + 3$, 17). Exact mass for $C_{132}H_{150}N_{12}O_4$: calculated 1967.1902, found 1967.1974.

5,15-Bis(4′-(15″-(2‴-(1‴,4‴-benzoquinonyl))-2″,8″,12″,18″-tetraethyl-3″,7″,13″,17″-tetramethylporphyrinyl)phenyl)-2,8,12,18-tetrabutyl-3,7,13,17-tetramethylporphyrin (3). The protected bis-hydroquinone trimer, **17**, (50 mg, 0.022 mmol) was stirred in 10 mL of freshly distilled CH_2Cl_2 and purged with Ar for 15 min. A freshly prepared solution of BI_3 (1.3 mL of a 0.81 M solution in CH_2Cl_2) was added dropwise over a 30-s addition time at 0 °C. The reaction was allowed to stir in the dark at 0 °C for 15 min. At this time, the vessel was removed from the ice bath and warmed to room temperature for 30 min. Excess BI_3 was quenched with H_2O and the reaction neutralized with dilute ammonia. The organic layer was separated and dried over Na_2SO_4, and the solvent removed under reduced pressure to a volume of approximately 50 mL. DDQ (25 mg, 0.11 mmol) was added and the reaction stirred at room temperature, in the dark, for 2.5 h. The reaction mixture was washed with aqueous Na_2CO_3 and H_2O and dried over Na_2SO_4. The product, **3**, was purified by column chromatography on silica gel (2% MeOH/$CHCl_3$ eluent) to yield 16.9 mg (0.0089 mmol, 41% yield) of a pale burgundy solid. UV–vis ($CHCl_3$): λ_{max} 414, 510, 541, 575, 626 nm. ^{1}H NMR (300 MHz, $CDCl_3$): δ −1.99 (2H, s, N*H*), −1.88 (2H, s, N*H*), −1.46 (2H, s, N*H*), 1.28 (12H, t, 2,8,12,18-$CH_2CH_2CH_2CH_3$), 1.88–1.97 (32H, m, 2,8,12,18-$CH_2CH_2CH_2CH_3$ and 2″,8″,12″,18″-CH_2CH_3), 2.39 (8H, q, 2,8,12,18-$CH_2CH_2CH_2CH_3$), 3.09 (24H, s, 3,7,13,17-CH_3, 3″,7″-CH_3), 3.17 (12H, s, 13″,17″-CH_3), 4.14–4.23 (24H, m, 2″,8″,12″,18″-CH_2CH_3 and 2,8,12,18-$CH_2CH_2CH_2CH_3$), 7.34 (8H, dd, 2′,3′-*H*), 8.42 (6H, m, quinone-*H*), 10.39 (4H, s, 10″,20″-*H*), 10.49 (2H, 10,20-*H*) ppm. ^{13}C NMR (500 MHz, $CDCl_3$): δ 14.39, 16.37, 17.33, 17.49, 17.71, 20.04, 20.11, 23.60, 26.82, 29.70, 35.71, 97.23, 97.39, 110.23, 117.94, 119.28, 133.31, 133.38, 133.50, 135.92, 136.13, 137.17, 137.93, 139.53, 141.17, 141.24, 141.33, 141.96, 142.26, 143.46, 144.67, 144.90, 145.71, 146.05, 187.34, 189.00 ppm. Mass spectrum (FAB, 70 eV): *m/z* (relative intensity, %) 1909 (M^+, 57), 1910 ($M^+ + 1$, 100), 1911 ($M^+ + 2$, 73), 1912 ($M^+ + 3$, 49). Anal. Calcd for $C_{128}H_{138}N_{12}O_4 \cdot 2H_2O$: C, 79.06; H, 7.36; N, 8.64. Found: C, 79.32; H, 7.29; N, 8.59.

5-(4′-(5‴-(13‴,17‴-Dibutyl-2‴,8‴-diethyl-3‴,7‴,12‴,18‴-tetramethylporphyrinyl))phenyl)-15-(4″-(5‴-(15‴-(2‴″,5‴″-dimethoxyphenyl)-2‴″,8‴″,12‴″,18‴″-tetraethyl-3‴″,7‴″,13‴″,17‴″-tetramethylporphyrinyl))phenyl)-2,8,12,18-tetrabutyl-3,7,13,17-tetramethylporphine (18). A 100-mL, three-necked, round-bottomed flask equipped with an argon inlet and a septum port was charged with **14** (120 mg, 0.187 mmol, 10^{-2} M), **15** (134 mg, 0.187 mmol, 10^{-2} M), **16** (107 mg, 0.375 mmol, 2×10^{-2} M), and 37.5 mL of freshly distilled CH_2Cl_2. The solution was bubbled with argon for 15 min and covered with aluminum foil. Trifluoroacetic acid (29 μL, 10^{-3} M) was added, and the reaction was stirred in the dark under an argon atmosphere for 3.5 h; after this time, *o*-chloranil (138 mg) was added and the reaction allowed to stir overnight. The contents of the reaction were poured into K_2CO_3(aq) and extracted several times with CH_2Cl_2. The organic phase was washed with H_2O and dried over Na_2SO_4, and the solvent was removed on a rotary evaporator to yield a dark solid. The solid was dissolved in a minimum amount of a 2% MeOH/$CHCl_3$ and loaded onto silica gel. The three trimeric porphyrins could be separated from the starting materials by elution with 2% MeOH/$CHCl_3$. The desired product, **18**, was obtained pure by careful, repeated, chromatography on silica gel (1% MeOH/$CHCl_3$) followed by recrystallization from $CHCl_3$/hexanes to give 83 mg (0.044 mmol, 23% yield) of a deep red-violet solid. UV–vis ($CHCl_3$): λ_{max} 422, 508, 538, 575, 625 nm. ^{1}H NMR (300 MHz, $CDCl_3$): δ −2.96 (1H, s, N‴″*H*), −2.72 (1H, s, N‴″*H*), −1.96 (1H, s, N‴″*H*), −1.89 (1H, s, N‴″*H*), −1.47 (1H, s, N*H*), −1.43 (1H, s, N*H*), 1.09 (6H, t (J = 7.4 Hz), 13‴,17‴-$CH_2CH_2CH_2CH_3$), 1.26 (6H, t (J = 7.3 Hz), 2,8-$CH_2CH_2CH_2CH_3$), 1.27 (6H, t (J = 7.4 Hz), 12,18-$CH_2CH_2CH_2CH_3$), 1.48 (8H, m, 2,8,12,18-$CH_2CH_2CH_2CH_3$), 1.68 (4H, sextet (J = 7.4 Hz), 13‴,17‴-$CH_2CH_2CH_2CH_3$), 1.94 (18H, m, 2‴″,8‴″- and 2‴″,8‴″,12‴″,18‴″-CH_2CH_3), 2.20 (4H, quintet (J = 7.4 Hz), 13‴,17‴-$CH_2CH_2CH_2CH_3$), 2.38 (8H, m, 2,8,12,18-$CH_2CH_2CH_2CH_3$), 2.70 (6H, s, 13‴″,17‴″-CH_3), 2.97 (12H, s, 13,17,3‴″,7‴″-CH_3), 2.99 (6H, s, 3,7-CH_3), 3.02 (6H, s, 3‴″,7‴″-CH_3), 3.66 (6H, s, 12‴″,18‴″-CH_3), 3.73 (3H, s, 5‴″-OCH_3), 3.82 (4H, t (J = 7.6 Hz), 13‴″,17‴″-$CH_2CH_2CH_2CH_3$), 3.87 (3H, s, 2‴″-OCH_3), 4.21 (20H, m, 2,8,12,18-$CH_2CH_2CH_2CH_3$, 2‴″,8‴″-CH_2CH_3, and 2‴″,8‴″,12‴″,18‴″-CH_2CH_3), 7.30 (1H, s, 4‴″-*H*), 7.35 (2H, d, 1‴″,6‴″-*H*), 8.16 (8H, m, 2′,3′,2″,3″-*H*), 9.62 (1H, s, 15‴-*H*), 10.29 (2H, s, 10‴″,20‴″-*H*), 10.38 (2H, s, 10‴″,20‴″-*H*), 10.49 (2H, s, 10,-20-*H*) ppm. ^{13}C NMR (300 MHz, $CDCl_3$): δ 11.7, 11.8, 13.6, 14.0, 14.1, 14.2, 14.3, 14.4, 17.6, 17.7, 17.8, 20.0, 20.1, 22.9, 23.1, 23.2, 23.6, 25.9, 26.8, 29.7, 34.3, 35.1, 35.2, 35.7, 56.0, 56.1, 96.5, 96.6, 96.7, 97.2, 111.9, 115.0, 17.7, 118.8, 120.3, 132.6, 132.7, 132.9, 133.0, 135.2, 135.5, 135.7, 135.9, 135.9, 136.2, 136.3, 140.1, 140.4, 140.7, 140.8, 141.0, 141.1, 141.2, 141.3, 141.6, 141.8, 141.9, 143.0, 143.0, 143.6, 143.9, 144.2, 144.4, 144.5, 144.6, 144.8, 144.9, 145.4, 145.5, 145.8, 153.9 ppm. Mass spectrum (FAB, 70 eV): *m/z* (relative intensity, %) 1893 ($M^+ + 4$, 50), 1892 ($M^+ + 3$, 65), 1891 ($M^+ + 2$, 59), 1890 ($M^+ + 1$, 100), 1889 (M^+, 67). Exact mass for $C_{128}H_{151}N_{12}O_2$: calcd 1888.2083, obsd. 1888.2075.

5-(4′-(5‴-(13‴,17‴-Dibutyl-2‴,8‴-diethyl-3‴,7‴,12‴,18‴-tetramethylporphyrinyl))phenyl)-15-(4″-(5⁗-(15⁗-(2⁗⁗-(1⁗⁗,4⁗⁗-benzoquinonyl))-2⁗⁗,8⁗⁗,12⁗⁗,18⁗⁗-tetraethyl-3⁗⁗,7⁗⁗,13⁗⁗,17⁗⁗-tetramethylporphyrinyl))phenyl)-2,8,12,18-tetrabutyl-3,7,13,17-tetramethylporphine (2). A 100-mL round-bottomed flask, equipped with a side arm, was charged with **18** (177 mg, 0.094 mmol), a stir bar, and 28 mL of CH_2Cl_2 (freshly distilled from CaH). The flask was shielded from ambient lighting and placed in an ice/water bath, and the solution purged with Ar for 15 min. At this time, 1.97 mL of a 0.81 M solution (1.6 g in 5 mL of CH_2Cl_2) of BI_3 was added *via* syringe with an addition time of 2 min. After the addition was complete, the flask was removed from the ice/water bath, and the solution was allowed to stir at room temperature for 30 min. Excess BI_3 was quenched with H_2O and the reaction neutralized with aqueous NH_3. The contents were then placed into a separatory funnel and partitioned between H_2O and CH_2Cl_2. The CH_2Cl_2 solution was washed thoroughly with H_2O, dried over Na_2SO_4, and evaporated to dryness on a rotary evaporator. At this point the *hydroquinone* was not isolated, but rather, taken up with 20 mL of a 2% MeOH/$CHCl_3$ (v/v) solution and treated with 62 mg of DDQ and 1 drop of Et_3N for 30 min. The desired product was purified by column chromatography on silica gel (2% MeOH/$CHCl_3$ eluent) and recrystallized from $CHCl_3$/hexanes in a vapor diffusion chamber to yield 138 mg of **2** (0.074 mmol, 79% yield) as a dark burgundy solid. UV–vis ($CHCl_3$): λ_{max} 411, 508, 538, 575, 625 nm. ^{1}H NMR (300 MHz, $CDCl_3$): δ −2.98 (2H, s, N‴-*H*), −1.92 (2H, s, N⁗-*H*), −1.46 (2H, s, N-*H*), 0.97 (6H, t (J = 7.3 Hz), 13‴,17‴-$CH_2CH_2CH_2CH_3$), 1.25 (6H, t (J = 7.4 Hz), 2,8-$CH_2CH_2CH_2CH_3$), 1.29 (6H, t (J = 7.4 Hz), 12,18-$CH_2CH_2CH_2CH_3$), 1.49 (8H, m, 2,8,12,18-$CH_2CH_2CH_2CH_3$), 1.68 (4H, sextet (J = 7.4 Hz), 13‴,17‴-$CH_2CH_2CH_2CH_3$), 1.91 (18H, m, 2‴,8‴- and 2⁗,8⁗,12⁗,18⁗-CH_2CH_3), 2.20 (4H, quintet (J = 7.4 Hz), 13‴,-17‴-$CH_2CH_2CH_2CH_3$), 2.38 (8H, m, 2,8,12,18-$CH_2CH_2CH_2CH_3$), 2.70 (6H, s, 13⁗,17⁗-CH_3), 2.97 (12H, s, 13,17,3⁗,7⁗-CH_3), 2.99 (6H, s, 3,7-CH_3), 3.02 (6H, s, 3‴,7‴-CH_3), 3.66 (6H, s, 12‴,18‴-CH_3), 3.73 (3H, s, 5⁗-OCH_3), 3.82 (4H, t (J = 7.6 Hz), 13‴,17‴-$CH_2CH_2CH_2CH_3$), 3.87 (3H, s, 2⁗-OCH_3), 4.21 (20H, m, 2,8,12,18-$CH_2CH_2CH_2CH_3$, 2‴,8‴-CH_2CH_3, and 2⁗,8⁗,12⁗,18⁗-CH_2CH_3), 7.30 (1H, s, 4⁗-*H*), 7.35 (2H, d, 1⁗,6⁗-*H*), 8.16 (8H, m, phenyl-*H*), 9.32 (1H, s, 15‴-*H*), 10.28 (2H, s, 10‴,20‴-*H*), 10.41 (2H, s, 10⁗,20⁗-*H*), 10.49 (2H, s, 10,20-*H*) ppm. ^{13}C NMR (300 MHz, $CDCl_3$): δ 11.6, 11.7, 13.8, 13.9, 14.4, 16.3, 16.5, 16.7, 16.9, 17.7, 17.8, 20.1, 22.7, 22.8, 23.7, 25.5, 26.9, 34.8, 35.0, 35.8, 35.8, 95.0, 96.4, 97.1, 97.2, 106.3, 117.5, 117.6, 118.7, 118.8, 131.9, 132.1, 132.2, 132.3, 133.2, 135.5, 135.6, 135.8, 137.1, 137.8, 139.4, 139.9, 140.0, 140.5, 140.6, 141.0, 141.1, 141.4, 141.5, 142.7, 142.8, 143.5, 143.7, 144.3, 144.5, 144.7, 145.5, 145.6, 145.7, 150.0, 187.2, 188.9 ppm. Mass spectrum (FAB, 70 eV): m/z (relative intensity, %) 1858 (M^+, 21), 1859 (M^+ + 1, 35), 1860 (M^+ + 2, 78), 1861 (M^+ + 3, 100), 1862 (M^+ + 4, 63), 1863 (M^+ + 5, 31). Exact mass for $C_{126}H_{145}N_{12}O_2$: calcd 1858.1613, obsd 1858.1608. Anal. Calcd for $C_{126}H_{145}N_{12}O_2 \cdot H_2O$: C, 80.60; H, 7.89; N, 8.95. Found: C, 80.50; H, 7.92; N, 8.95.

Acknowledgment. This work was supported by the Robert A. Welch Foundation, the Camille and Henry Dreyfus Foundation (Teacher-Scholar Award to J.L.S.), the National Institutes of Health (Grant GM41657 to J.L.S.), and the National Science Foundation (Grant CHE 9102657 to A.H.). The Center for Fast Kinetics Research is supported jointly by the Biotechnology Research Resources Division of the the National Institutes of Health (Grant RR00886) and by the University of Texas at Austin.